Quantum Erasure
SK2903 - Quantum Technology

Arpit Sharma

February 1, 2025

Abstract

This experiment investigates the quantum eraser phenomenon, a fundamental concept in quantum mechanics that demonstrates the connection between interference and the distinguish-ability of quantum states. Utilizing a source of photon pairs based on spontaneous parametric down-conversion (SPDC) and a Michelson interferometer, the experiment explores the interference patterns of photons under different polarization settings. The results demonstrate the loss of interference when the photon paths are made distinguishable and the recovery of interference when distinguish-ability is erased by manipulating the polarization states. By analyzing the visibility and distinguish-ability of the interference patterns, the experiment highlights the subtle interplay between measurement, complementarity, and entanglement in quantum mechanics.

1 Introduction

The quantum eraser experiment is a profound demonstration of quantum mechanical principles, showcasing the intricate relationship between interference, distinguishability, and measurement. It challenges classical notions of probability and underscores the wave-particle duality of light. At the heart of the experiment lies the concept of quantum interference, where the probability of detecting a photon at a specific location depends on the superposition of multiple possible paths it could have taken.

In a Mach-Zehnder interferometer, for instance, a photon can traverse either arm A or arm B, and its state can be described as a superposition of these two possibilities:

$$|\psi_1> = \frac{1}{\sqrt{2}}(|A> + |B>)$$

This equation represents the initial state of the photon before entering the interferometer. The amplitudes for each path are equal because the interferometer uses a 50:50 beam splitter.

A phase difference can be introduced between the paths by making one arm slightly longer. Considering arm B is longer and induces a phase $e^{i\phi}$, the state becomes:

$$|\psi_2> = \frac{1}{\sqrt{2}}(|A> + e^{i\phi}|B>)$$

After the photon passes through the second beam splitter, the state can be written as:

$$|\psi_3> = \frac{1}{2}((1 + e^{i\phi})|A> + (1 - e^{i\phi})|B>)$$

The probability of detecting the photon at the exit path $|B>$ is then given by the squared norm of the corresponding amplitude:

$$P(det.) = |\frac{1}{2}(1 - e^{i\phi})|^2 = \frac{1}{2}(1 - \cos\phi)$$

This equation demonstrates the interference term $\frac{1}{2}\cos\phi$. The probability of detecting the photon oscillates with the phase difference between the two paths, giving rise to the interference pattern.

When the photon's path becomes distinguishable, the interference pattern vanishes, reflecting the principle of complementarity. This can be done by assigning orthogonal polarizations to the paths—horizontal ($|H\rangle$) for arm A and vertical ($|V\rangle$) for arm B. Even without directly measuring polarization, the mere distinguishability eliminates interference.

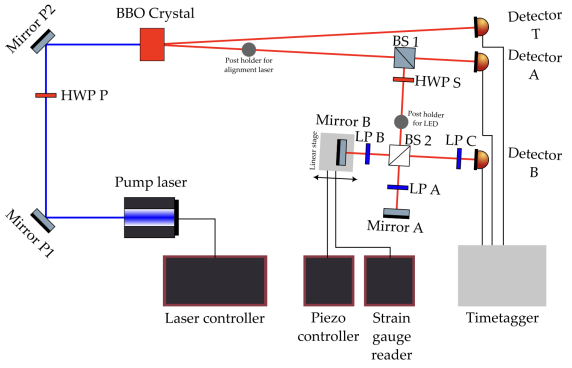

Figure 1: **Schematic diagram of the setup used to observe quantum erasure**.[1]

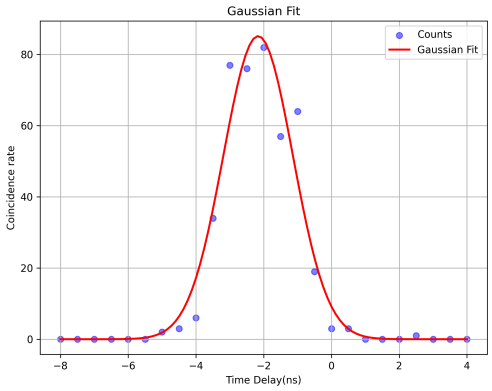

Figure 2: **Coincidence rate vs time delay**. Gaussian curve was fit over coincidence rate.

Interference can be restored by erasing the "which-path" information, such as by placing a diagonal polarizer ($|D\rangle = \frac{1}{\sqrt{2}}(|H\rangle + |V\rangle)$) before the detector, making the paths indistinguishable. This quantum eraser phenomenon demonstrates the role of measurement in quantum mechanics.

The experiment uses photon pairs from SPDC and a Michelson interferometer with polarizers to explore the quantum eraser effect, revealing the interplay between visibility and path distinguishability.

2 Measurements

2.1 Coincidence Settings

Data was collected to optimize the delay and coincidence window width for maximizing the signal-to-noise ratio (SNR) while maintaining a high coincidence rate. With arm B blocked, the delay between detectors B and T was scanned from -8 ns to 4 ns using a 1 ns coincidence window to identify the optimal delay (Δt) (see fig. 2).

Accidental coincidences rate, Coincidence rate and SNR were then measured by setting $\Delta t = -2.5$ ns, and the coincidence window width was varied from 1 ns to 6 ns. An optimal value was selected for the coincidence window to balance SNR and coincidence rate, finalizing the calibration. The collected data can be seen in the fig. 3.

2.2 Coherence measurements

To study the interference properties of SPDC photons, we analyzed interferograms. A scan between 9 µm and 11 µm with a 70 nm step revealed oscillations in coincidence rates with a 400 nm period, matching the wavelength of the light source. When moving the fine adjuster, we observed changes in the interference fringes' intensity, with small adjustments causing large swings in intensity. Adjusting the kinematic screws on mirror A affected the alignment, altering the visibility and shifting the fringe pattern. Proper alignment was achieved when small fine adjuster movements caused significant intensity changes without visible fringes on the screen. Fig. 4 shows one of

We then varied the fine adjuster position from -60 μm to $+50$ μm in 10 µm steps, recording the maximum ($C_{\max}$) and minimum ($C_{\min}$) coincidence rates to calculate visibility ($V = \frac{C_{\max}-C_{\min}}{C_{\max}+C_{\min}}$). The optimal fine adjuster position, yielding the highest visibility, was identified. Visibility decreased as the adjuster moved away from this point, confirmed by plotting visibility against the stage position.

2.3 Quantum erasure measurements

For the third task of the experiment, we calculated Visibility (V), Distinguishability (D), and M as a function of the Linear Polarizer (LP) C angle, which was varied in discrete steps of 15°,

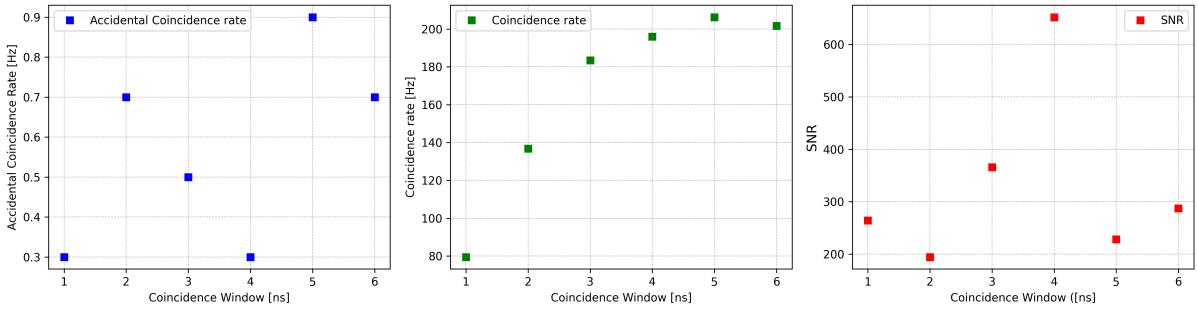

Figure 3: **Accidental coincidence rate, Coincidence rate and SNR plotted against coincidence window**.

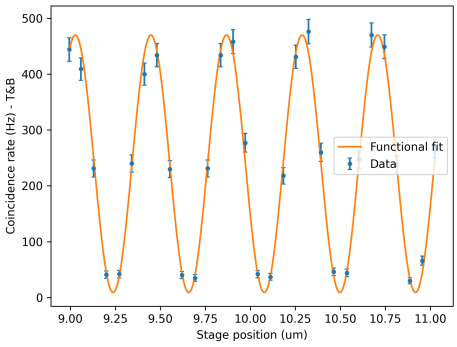

Figure 4: **Interference pattern**.

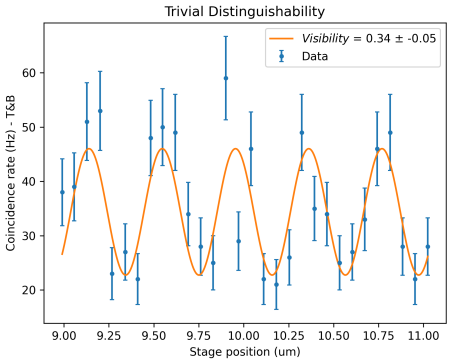

Figure 6: **Trivial Distinguishability**.

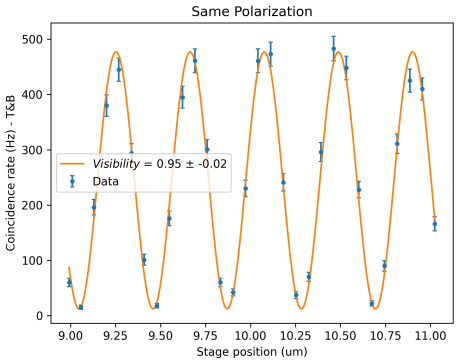

Figure 5: **Same Polarization**.

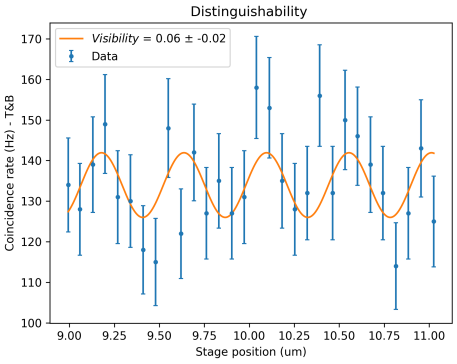

Figure 7: **Distinguishability**.

covering the range from 0° to 90°. Before starting the measurements, adjustments to the Half-Wave Plate (HWP) labeled S were made to balance the coincidence rate. This was done by alternately blocking the two arms of the Michelson interferometer and identifying an angle *alpha* of the HWP S that achieved the balance. Once this condition was met, HWP S was rotated to the angle *alpha*, LP A was set to 0°, and LP B was set to 90°. With these settings in place, the standard measurement

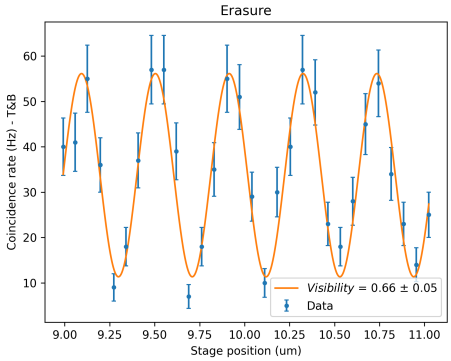

Figure 8: **Erasure**.

Figure 9: **Accidental coincidences vs window**.

procedure was carried out. The four initial interferograms (same polarization, trivial distinguishability, distinguishability, erasure) can be seen in the fig. 5 6 7 8 respectively. The recorded data was organized in the excel sheet provided for the calculations of Visibility, Distinguishability, and M for each LP C angle using a photodetector setup. We recorded the maximum visibility when the LP C was at angle 45° and the distinguishability was minimum at this point.

3 Analysis

3.1 Coincidence Settings

In Fig. 2, the coincidence rate peaks near $-2.5\ ns$, which we select to maximize the capture of true coincident events while minimizing timing misalignment.

With the time delay fixed, the coincidence window is varied to find the optimal duration, as shown in Fig. 3. The coincidence rate initially increases with the window width, capturing more true and accidental coincidences, but the growth slows as most true coincidences are already included within a smaller window.

A reduced count in detector B, due to a partially closed iris, caused slight fluctuations in the accidental coincidence rate and SNR curves (Fig. 3a & 3c). However, we still see a general trend of linear increase in acc. coincidence rate with increase in the coincidence window following the relation $R_{\text{acc}} = R_B R_T \tau$, where R_B & R_T are detection rates for T and B detectors and τ is a coincidence window.

Comparing experimental and expected accidental rates (Fig. 9), the experimental data deviates slightly in some cases but aligns well with the expected linear trend after fitting.

The optimal coincidence window width balances high SNR with capturing true coincidences. In our setup, the SNR is highest, and accidental coincidences are minimized at 4 ns, which we choose as the coincidence window.

3.2 Coherence measurements

We measure the visibility of interference patterns from multiple interferograms. For each interferogram, the data for coincidence rates were fitted with a *sine* function using python module scipy[2] to identify the maximum ($C_{\max}$) and minimum ($C_{\min}$) coincidence rates. The visibility was calculated using the formula $V = \frac{C_{\max} - C_{\min}}{C_{\max} + C_{\min}}$.

One representative interferogram plotted alongside its sine fit can be seen in fig. 4. To analyze the visibility decay further, the visibility was plotted as a function of the stage position, corresponding to the difference in optical path length between the two arms of the Michelson interferometer.

The visibility exhibited a peak at the central position and decayed symmetrically as the optical path difference increased. The expected functional form of visibility is a *sinc* function. This is because the visibility is the modulus of the coherence function, which is the Fourier transform of the power spectrum, and the power spectrum is a rectangular function whose Fourier transform is a *sinc* function. Therefore, we fit the data to a *sinc* function of the form $V(t) \sim |\text{sinc}\left(\frac{\Delta\omega}{2}t\right)|$.

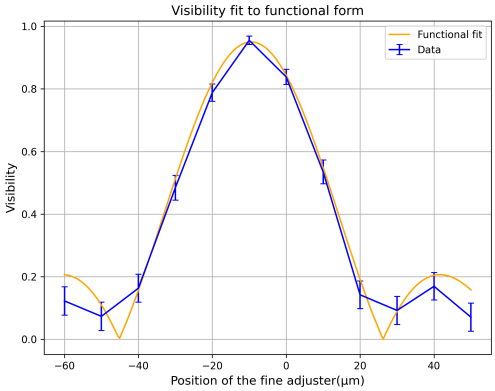

Figure 10: Visibility as a follows as symmetric .

3.3 Quantum erasure measurements

The quantum eraser experiment successfully demonstrated the manipulation of interference visibility by controlling the distinguishability of photon paths. The initial interferograms, obtained under varying polarization conditions, clearly showed the loss and recovery of interference as distinguishability was introduced and subsequently erased (see fig. 11). When the paths were indistinguishable (same polarization), strong interference was observed with high visibility. Introducing orthogonal polarizations in the two arms led to a loss of interference and reduced visibility. However, by erasing the polarization information with a properly oriented LP C, interference was recovered, leading to increased visibility.

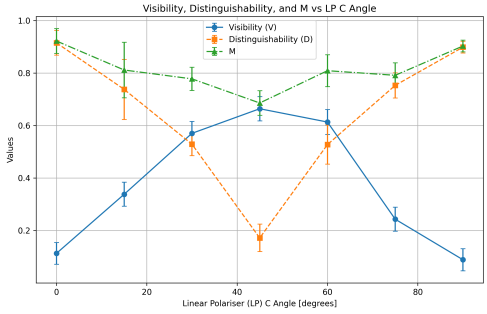

Figure 11: **Figure shows visibility, distinguishability and M parameter against the angle of LP C.**

Further analysis involved measuring interferograms and coincidence rates for different angles of LP C. The plots of visibility (V) and distinguishability (D) against the LP C angle revealed a clear trade-off between these two quantities. V exhibited an oscillating pattern, peaking when LP C erased distinguishability, while D showed an opposite trend, maximizing when distinguishability was maximized. The M parameter, calculated as $\sqrt{V^2 + D^2}$, remained relatively constant, confirming the complementary relationship between V and D as predicted by theory.

4 Conclusion

This experiment successfully demonstrated the quantum eraser concept, highlighting the intricate relationship between interference visibility, distinguishability, and quantum measurements. We utilized a source of photon pairs based on spontaneous parametric down-conversion and a Michelson interferometer to manipulate and observe these phenomena. By adjusting the polarization states in the interferometer arms, we controlled the distinguishability of the photon paths, leading to a predictable modulation of the interference visibility. The initial interferograms confirmed that when the paths were indistinguishable, strong interference was observed, while introducing distinguishability through orthogonal polarizations resulted in a loss of interference.

Crucially, we demonstrated the quantum eraser effect by erasing the distinguishability information using a carefully oriented linear polarizer, which led to a recovery of the interference pattern. Further analysis revealed a clear trade-off between visibility (V) and distinguishability (D) as a function of the polarizer angle, confirming their complementary nature. The ability to control and erase information, as demonstrated in this experiment, holds significant potential for various quantum technologies, including quantum communication, computing, and imaging.

5 Methods

The python code used to analyse the data and perform curve fitting can be found in the jupyter notebook present here.

References

[1] Lab Manual Quantum Eraser for Quantum Technology. Giulio Foletto. (2024)

[2] https://docs.scipy.org/doc/scipy/reference/tutorial/curve_fit.html